

## Article

# Improving the Quality of Spontaneously Growing HviGH11 Crystals by Increasing the Viscosity Using Polyethylene Glycols

Ki Hyun Nam 

College of General Education, Kookmin University, Seoul 02707, Republic of Korea; structure@kookmin.ac.kr

**Abstract:** Proteins can form crystals spontaneously without crystallization experiments. These crystals can be used to determine three-dimensional structures. However, when X-ray diffraction is poor, crystal optimization is required to obtain a high-resolution crystal structure. Endo-1,4- $\beta$ -xylosidase from the fungus *Hypocrea virens* (HviGH11) spontaneously formed microcrystals after affinity purification and concentration; however, most HviGH11 microcrystals showed poor diffraction in the synchrotron X-ray and X-ray free-electron laser, so a complete three-dimensional structure could not be obtained. This study presents a method to improve the crystal quality of spontaneously grown HviGH11 microcrystals. The crystallization screening results revealed that temperature, pH, and salt were not crucial factors in increasing the solubility or preventing the spontaneous crystal growth of HviGH11. Conversely, the addition of polyethylene glycols (PEGs) as a precipitant facilitated the growth of larger HviGH11 crystals. The improved large HviGH11 crystal showed a diffraction of up to 1.95 Å when exposed to synchrotron X-rays, providing a complete three-dimensional structural dataset. Based on the nucleation rate equation, it was suggested that PEG increases the viscosity of the protein solution rather than promoting nucleation. This increase in viscosity reduced nucleation and facilitated the growth of larger HviGH11 crystals. These results provide valuable insights for future experiments aimed at increasing the size of spontaneously grown crystals.

**Keywords:** spontaneously grown crystal; crystallization; optimization; viscosity; xylanase; HviGH11



**Citation:** Nam, K.H. Improving the Quality of Spontaneously Growing HviGH11 Crystals by Increasing the Viscosity Using Polyethylene Glycols. *Crystals* **2024**, *14*, 289. <https://doi.org/10.3390/crust14030289>

Academic Editor: Borislav Angelov

Received: 5 March 2024

Revised: 15 March 2024

Accepted: 20 March 2024

Published: 21 March 2024



**Copyright:** © 2024 by the author. Licensee MDPI, Basel, Switzerland. This article is an open access article distributed under the terms and conditions of the Creative Commons Attribution (CC BY) license (<https://creativecommons.org/licenses/by/4.0/>).

## 1. Introduction

In macromolecular crystallography (MX), high-quality crystals are essential for obtaining diffraction data to determine three-dimensional structures [1]. In the general experimental procedure, recombinant or naturally derived proteins are purified and crystallization experiments are performed to obtain crystal samples [2,3]. In contrast, the spontaneous crystallization of various proteins has been reported in nature [4,5]. A prime example is the spontaneous growth of myoglobin crystals, which marked the beginning of protein crystallography [4]. Furthermore, proteins such as Bt toxins [6], calcineurin [7], pea legumin A [8], human immunoglobulin G2 [9], cathepsin B [10], neuraminidase [10], polyhedrin [11], fusolin [12], luciferase [13], BinAB [14], and granulin [15] naturally form crystals in cells. These spontaneously grown crystals are used to collect diffraction data to determine protein structures. Most previous studies have used a synchrotron X-ray source to obtain diffraction data from spontaneously grown crystals [4,10–12], but when the crystals are small or the diffraction intensity is weak, diffraction data have been collected using an intense X-ray free-electron laser (XFEL) [14–16]. If these spontaneously generated crystals do not have the sufficient diffraction limit to determine the crystal structure, even under intense X-rays, crystal optimization experiments must be carried out.

Endo-1,4- $\beta$ -xylosidase GH11 hydrolyzes the  $\beta$ -1,4 bonds in plant xylan and decomposes the linear polysaccharide xylan into xylose [17–20]. Because it can break down the second most naturally occurring renewable polysaccharide on Earth, it is a very important enzyme from the perspective of alternative energy sources [19,21]. Moreover, this enzyme is used in various industries such as pulp and paper bleaching, food, feed, and

pharmaceuticals [22,23]. The expression, crystallization, and preliminary XFEL diffraction of GH11 from the fungus *Hypocrea virens* (HviGH11) have been reported [24]. HviGH11 spontaneously crystallized into microcrystals in the microtube after Ni-NTA affinity chromatography and protein concentration. The dimensions of the spontaneously crystallized HviGH11 were approximately  $5 \times 5 \times 25 \mu\text{m}^3$  [24]. However, these microcrystals exhibited poor diffraction when exposed to synchrotron X-rays, making it impossible to collect three-dimensional structural information. Furthermore, when HviGH11 microcrystals were exposed to an intense X-ray free-electron laser (XFEL) to collect diffraction data, crystals were diffracted with a resolution of up to 2.3 Å, but most crystals showed poor or no diffraction. The phase problem was solved using 956 diffraction patterns of HviGH11; however, a complete dataset to determine the crystal structure was not collected. Therefore, improving the crystal quality and size is essential for determining the three-dimensional crystal structure of HviGH11.

To collect the complete diffraction dataset, crystal optimization was performed for spontaneously growing HviGH11 crystals. It was found that the temperature, pH, and salt conditions were not critical factors in preventing spontaneous crystal growth and optimizing crystal size. By adding the polyethylene glycol solution, suitable large HviGH11 crystals for X-ray diffraction were obtained. Using these optimized crystals, the complete three-dimensional structural datasets were acquired at a resolution of 1.95–2.40 Å. The possible crystallization mechanism to increase the size of spontaneously grown HviGH11 crystals using PEG agents was discussed. The results of this study will provide useful information for the crystal optimization of spontaneously growing protein crystals.

## 2. Materials and Methods

### 2.1. Protein Preparation

The protein expression and purification of HviGH11 have been previously reported [24]. Briefly, the recombinant DNA containing the N-terminal hexahistidine-tagged HviGH11 was transformed into *E. coli* BL21(DE3). The cells were grown in LB broth containing 50 µg/mL ampicillin at 37 °C. When the OD<sub>600</sub> reached 0.6–0.8, protein expression was induced by adding 0.5 mM isopropyl β-D-thiogalactopyranoside (IPTG) and conducting further incubation at 18 °C overnight. After cell lysis by sonication, cell debris was removed by centrifugation at 18,000× g for 1 h. The supernatant was loaded onto the Ni-NTA resin and washed with a buffer containing 50 mM Tris-HCl, pH 8.0, 200 mM NaCl, and 20 mM imidazole. HviGH11 was eluted using a buffer containing 50 mM Tris-HCl, pH 8.0, 200 mM NaCl, and 300 mM imidazole. The protein elution fractions were concentrated to 30 mg/mL using a protein concentrator (cutoff: 10,000 MW, Merck, Rahway, NJ, USA) for crystallization. The white aggregates generated during protein concentration were filtered using a 0.2 µm syringe filter (Korea Ace Scientific, Seoul, Republic of Korea). Protein concentration was measured by UV absorption at 280 nm using a NanoDrop 1000 spectrophotometer (Thermo Fisher Scientific, Waltham, MA, USA).

### 2.2. Crystallization and Crystal Optimization

In crystallization and crystal optimization experiments involving temperature, pH, salt, and PEG, the concentrated protein solution was centrifuged at 14,000 rpm and 4 °C for 15 min before crystallization experiments, and the supernatant was used for all crystallization experiments. To verify the reproducibility of the spontaneous crystallization of HviGH11, the protein solution (~30 mg/mL) was incubated at 4 °C overnight. To investigate the temperature effect, concentrated HviGH11 solution (~30 mg/mL) was incubated at room temperature (22–24 °C). For pH screening, the eluted HviGH11 solution after Ni-NTA purification was immediately diluted with 10 times the volume of acid (0.1 M MES, pH 6.0, and 200 mM NaCl) or alkaline (0.1 M CHES, pH 9.5, and 200 mM NaCl) solution. Each protein solution was concentrated using a concentrator and re-diluted 100 times with the same acidic and alkaline solution for a complete buffer change. The concentrated HviGH11 solution (~30 mg/mL) in acidic or alkaline solution was incubated at 4 °C overnight. To

examine the salt effect, protein purification was performed with buffers containing 20 mM, 500 mM, and 1 M NaCl during cell lysis and protein purification. After Ni-NTA purification, the protein solution was concentrated to ~30 mg/mL in different NaCl concentrations and incubated at 4 °C overnight. For the PEG effect, the high protein concentration solution (~30 mg/mL) was mixed with an equivalent volume of different PEGs (5–30% (*v/v*) PEG 400, 5–30% (*w/v*) PEG 4000 and PEG 8000) and incubated at 4 °C overnight. Protein solution and crystal screen solution mixtures were stored in 1.5 mL microcentrifuge tubes. After overnight incubation, the crystal suspension in a 1.5 mL microcentrifuge tube was pipetted very gently about 10 times using a micropipette and then transferred to a cover glass, and the HviGH11 crystallization drops were observed using an optical microscope.

### 2.3. X-ray Diffraction Data Collection

X-ray diffraction data were collected at beamline 11C at the Pohang Accelerator Laboratory (Pohang, Republic of Korea) [25]. The X-ray energy and photon flux were 12.658 keV (0.9794 Å) and  $\sim 5 \times 10^{11}$  photons per second. The beam size of the X-ray at the sample position was approximately 4 μm (vertical)  $\times$  8.5 μm (horizontal) full width at half maximum. For crystals obtained through a temperature, pH, and salt concentration screen, multiple microcrystals or relatively large crystals were soaked in a crystallization solution supplemented with 10–30% (*v/v*) glycerol or 10–30% (*v/v*) ethylene glycol for 5 s. Subsequently, the crystals were retrieved using a nylon loop, and they were mounted on a goniometer and subjected to X-ray diffraction experiments. For crystals obtained through the PEG screen, HviGH11 crystals were soaked for 5 s in a cryoprotectant solution containing a crystallization solution plus 30% (*v/v*) ethylene glycol. Data were collected in a cryogenic environment with a nitrogen gas stream at 100 K. The crystal-to-detector distance was 400 mm. X-ray diffractions were recorded with a PILATUS 6M detector (Dectris, Baden-Dättwil, Switzerland). Diffraction images were indexed, integrated, and scaled using the HKL2000 program [26]. Diffraction images were visualized using ALBULA (Dectris, Baden-Dättwil, Switzerland).

### 2.4. Structure Determination

The phase problem was solved with the molecular replacement method using MolREP (version 11.2.08) [27]. The search model structure was generated using AlphaFold2 [28]. Initial structure refinement was performed using REFMAC5 (version 5.8.0267) [29]. The model structure and electron density map of HviGH11 were visualized using PyMOL (version 2.4.1, DeLano Scientific LLC, San Carlos, CA, USA).

## 3. Results

### 3.1. Screening the Solubility of HviGH11

HviGH11 spontaneously grew into microcrystals after Ni-NTA affinity purification and concentration [24]. To verify whether the spontaneous crystallization process of HviGH11 was reproducible, the protein obtained after purification using Ni-NTA affinity chromatography was concentrated and stored at 4 °C. As shown in a previous study, a large number of HviGH11 microcrystals grew spontaneously in microtubes after overnight incubation (Figure 1A). The dimensions of these HviGH11 microcrystals were approximately  $5 \times 5 \times 20 \mu\text{m}^3$ . To reduce spontaneous crystal growth, the protein was diluted after Ni-NTA purification. However, when the concentration of HviGH11 was  $>3 \text{ mg/mL}$ , the microcrystals grew overnight, and this trend was the same as before [24]. At low HviGH11 solution concentrations  $<3 \text{ mg/mL}$ , no spontaneous crystal growth was observed, but some precipitation occurred after centrifugation. In addition, crystallization screening was performed with low protein concentrations ( $<1 \text{ mg/mL}$ ) after removal of the precipitate by centrifugation; however, only a few microcrystals were obtained, indicating that the protein concentration was insufficient to grow large crystals. Next, as with the crystal-seeding method, spontaneously grown microcrystals were added to the purified HviGH11 solution, but the crystal size did not increase significantly.

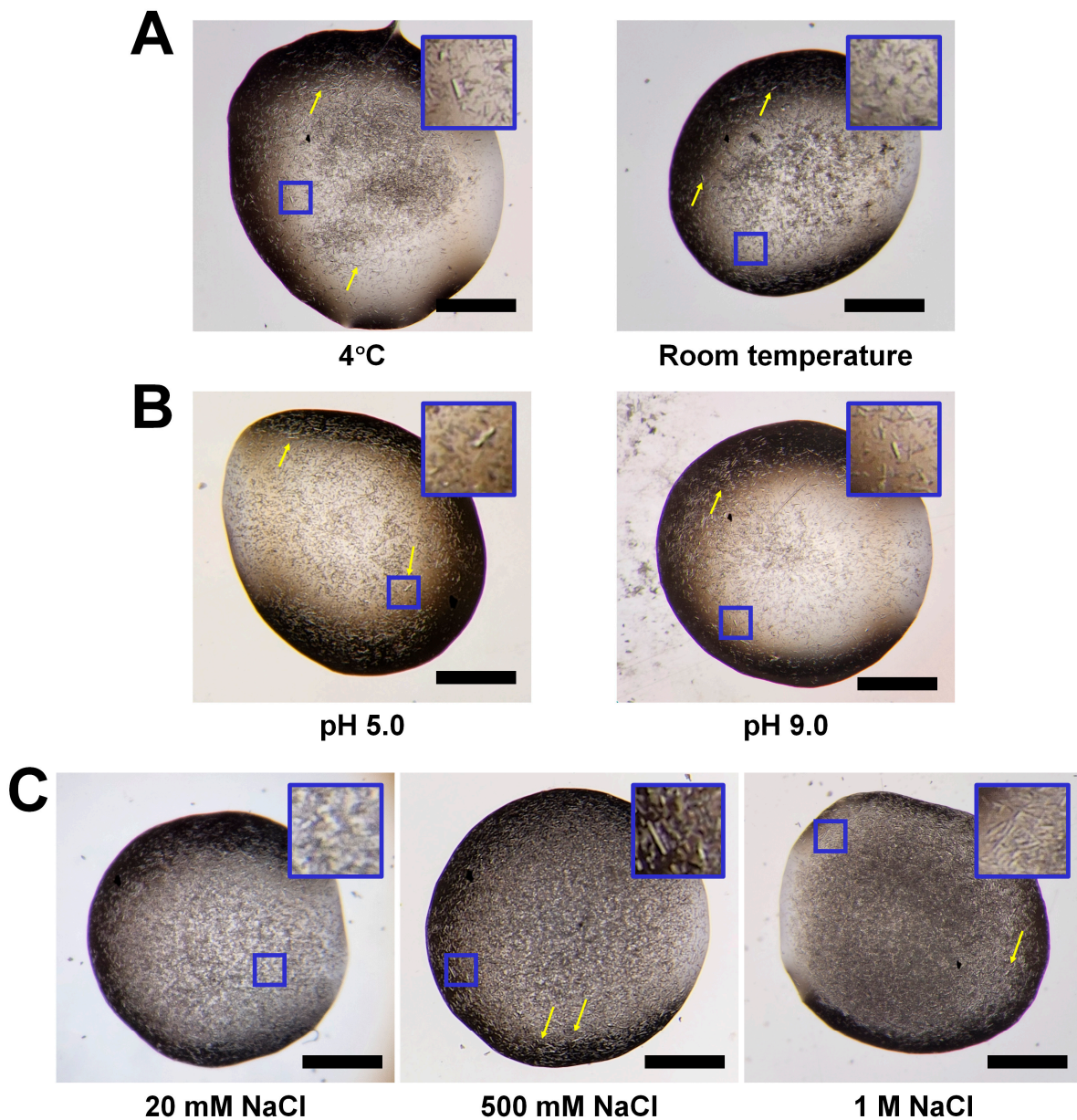


**Figure 1.** Solubility and crystal screening of HviGH11. Microscopic views of spontaneously grown HviGH11 microcrystals at different (A) temperatures, (B) pH values, and (C) NaCl concentrations. A close-up view of the small blue box displayed in the crystallization drop is shown at the top right of each figure. The relatively large crystals were indicated by yellow arrows. The scale bar indicates 500  $\mu\text{m}$ .

In general protein crystallization, temperature, pH, and salt concentration are important factors involved in nucleation and crystal growth [30]. Moreover, temperature, pH, and salt influence protein solubility [31]. Therefore, these factors can potentially hinder spontaneous crystal growth, allowing subsequent crystallization experiments to improve crystal size or quality.

To determine whether the temperature effect resulted in the prevention of spontaneous crystal growth and improvement of crystal size, purified HviGH11 was stored at room temperature. After overnight incubation at room temperature, HviGH11 microcrystals grew spontaneously (Figure 1A), suggesting that temperature changes are not a critical factor in preventing spontaneous crystal growth. The size of HviGH11 crystals spontaneously grown at room temperature was approximately  $5 \times 5 \times 20 \mu\text{m}^3$ , similar to incubation at  $4^\circ\text{C}$ .

pH is an important factor in protein solubility and can prevent protein aggregation by altering the net charge of the protein surface [32]. The pI of HviGH11 is 8.5. To

investigate the influence of pH on protein solubility, HviGH11 was stored in acidic (pH 6.0) or alkaline (pH 9.5) solution. To check the pH effect of preventing spontaneous crystal growth, concentrated HviGH11 solution was incubated at pH 6.0 and pH 9.5 at 4 °C. However, HviGH11 also spontaneously formed microcrystals with dimensions of approximately  $5 \times 5 \times 20 - 10 \times 10 \times 20 \mu\text{m}^3$  at pH 6.0 and pH 9.5 (Figure 1B). This result indicates that pH is not a critical factor preventing the spontaneous crystallization of HviGH11 and increasing the solubility.

Salt can disrupt protein–protein interactions in solutions and affect protein solubility [33]. However, high salt concentrations can reduce the electrostatic interactions between protein and solvent, leading to the aggregation or precipitation of less soluble or insoluble proteins [34]. To investigate the salt effect on solubility, HviGH11 was stored in buffer containing 20 mM, 500 mM, and 1 M NaCl during cell lysis and protein purification. After Ni-NTA purification, the HviGH11 solution was concentrated in different NaCl concentrations and incubated at 4 °C to examine where salt prevented spontaneous crystal growth. All HviGH11 solutions in different NaCl concentrations spontaneously crystallized (Figure 1C), suggesting that NaCl is not a crucial factor in preventing spontaneous crystallization; however, some HviGH11 crystal sizes slightly increased in 0.5 M and 1 M NaCl conditions, with dimensions of approximately  $15 \times 15 \times 30 \mu\text{m}^3$  (Figure 1C). These results indicate that NaCl can affect the size and thickness of HviGH11 crystals. Overall, the temperature, pH, and NaCl concentration used in this experiment were not crucial factors in increasing the solubility of HviGH11 to prevent spontaneous crystal growth.

Under the crystallization conditions obtained through the temperature, pH, and salt concentration screen, most HviGH11 crystals did not grow significantly. However, the quality of a crystal cannot be solely judged by its size observed under a microscope. Even if the crystals are not large enough, they have grown in a new crystallization screen environment, which can often affect protein packing and result in high diffraction intensities. Accordingly, small-sized HviGH11 crystals from various crystallization conditions were also exposed to X-rays to test the diffraction pattern, but the diffraction peaks were observed at low resolution in the range of 10–20 Å. Moreover, some relatively larger HviGH11 crystals (approximately  $15 \times 15 \times 40 \mu\text{m}^3$ ) were often observed in this experiment compared with crystals ( $5 \times 5 \times 25 \mu\text{m}^3$ ) used in previous crystallographic studies [24]. Using these relatively large crystals, an X-ray diffraction experiment was performed using synchrotron X-rays to test whether the relatively large crystal was suitable for collecting the three-dimensional diffraction dataset. However, the results showed that the highest diffraction peaks were observed at up to 7 Å with a low signal-to-noise ratio of < 3. All of these results indicate that spontaneously growing HviGH11 crystals obtained from the temperature, pH, and salt concentration screens are not suitable for X-ray diffraction experiments.

### 3.2. Improvement of HviGH11 Crystal by the Addition of PEGs

The spontaneous growth of HviGH11 crystals did not occur immediately after the protein was purified and took a long time. To identify the timing of HviGH11 microcrystal growth, crystal growth was monitored. Under a microscope, it was confirmed that a large number of HviGH11 microcrystals grew after approximately 2 h, but the size of the microcrystals stopped increasing after 5 h. The growth of a large number of microcrystals indicated that many crystal nuclei grew at a certain time in the concentrated HviGH11 solution. Accordingly, it was predicted that larger crystals would form if a small number of nucleation events were first induced by performing a crystallization experiment before generating many spontaneous nucleation events.

In previous solubility experiments, HviGH11 grew spontaneously without the influence of temperature, pH, or salt concentration. In particular, HviGH11 crystals grew spontaneously under the elution buffer composition of Ni-NTA purification, indicating that this buffer condition is suitable for HviGH11 nucleation. Accordingly, it was hypothesized that adding a precipitant before the spontaneous crystal growth process of HviGH11 could affect the amount of crystal nucleation or the nucleation rate, which could be a factor

influencing the crystal size. To verify this hypothesis, concentrated HviGH11 solution was mixed with PEG precipitant (10–30% (v/v) PEG 400 and 10–30% (w/v) PEG 4000 and PEG 8000) and incubated at 4 °C. As a result, larger HviGH11 crystals were obtained under all PEG conditions (Figure 2). These crystals had similar rod shapes regardless of PEG type and PEG concentration. The crystal size varied in the range of  $5 \times 5 \times 20$  –  $50 \times 50 \times 300 \mu\text{m}^3$ . As a result, the largest HviGH11 crystal size obtained in this experiment was approximately ten times larger than that of the previous spontaneously grown crystals.

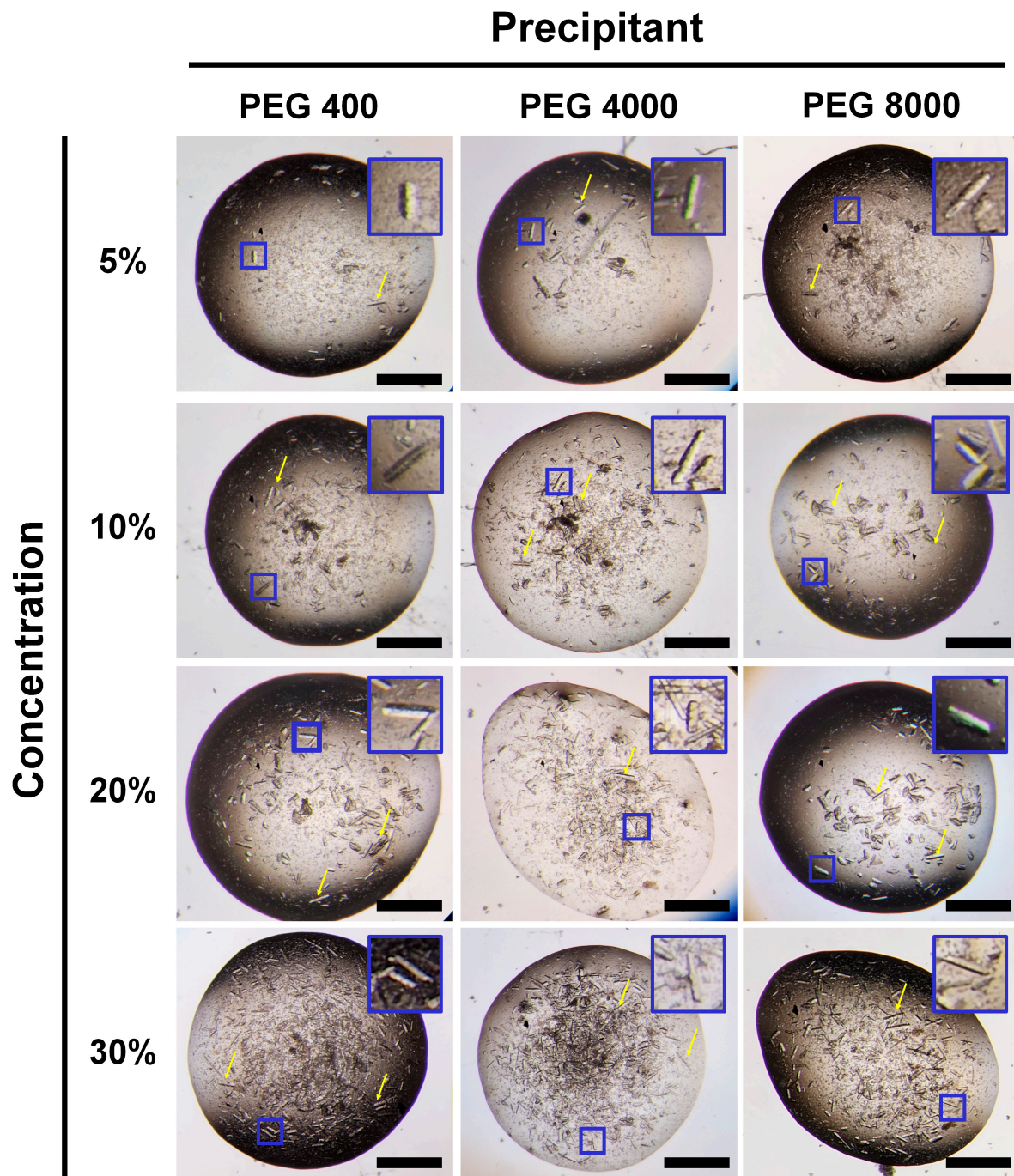


**Figure 2.** Photos of the crystal optimization of HviGH11 by adding PEG 400, PEG 4000, and PEG 8000. A close-up view of the small blue box displayed in the crystallization drop is shown at the top right of each figure. The relatively large crystals are indicated by yellow arrows. The scale bar indicates 500  $\mu\text{m}$ .

### 3.3. Verification of the Crystal Quality

To verify the quality of the large crystal size of HviGH11 obtained in this study, synchrotron X-ray diffraction experiments were performed (Figure 3A). All HviGH11 crystals grown by adding PEG 400, PEG 4000, and PEG 8000 showed good diffraction in the range of a 1.95–2.40 Å resolution (Figure 3B). The data processing results showed that all HviGH11 crystals belonged to orthorhombic  $P_{2_1}2_12_1$  space groups with similar unit cell dimensions (Table 1). This result showed that PEG precipitants were only involved in the nucleation of HviGH11 crystals and not in crystal packing.

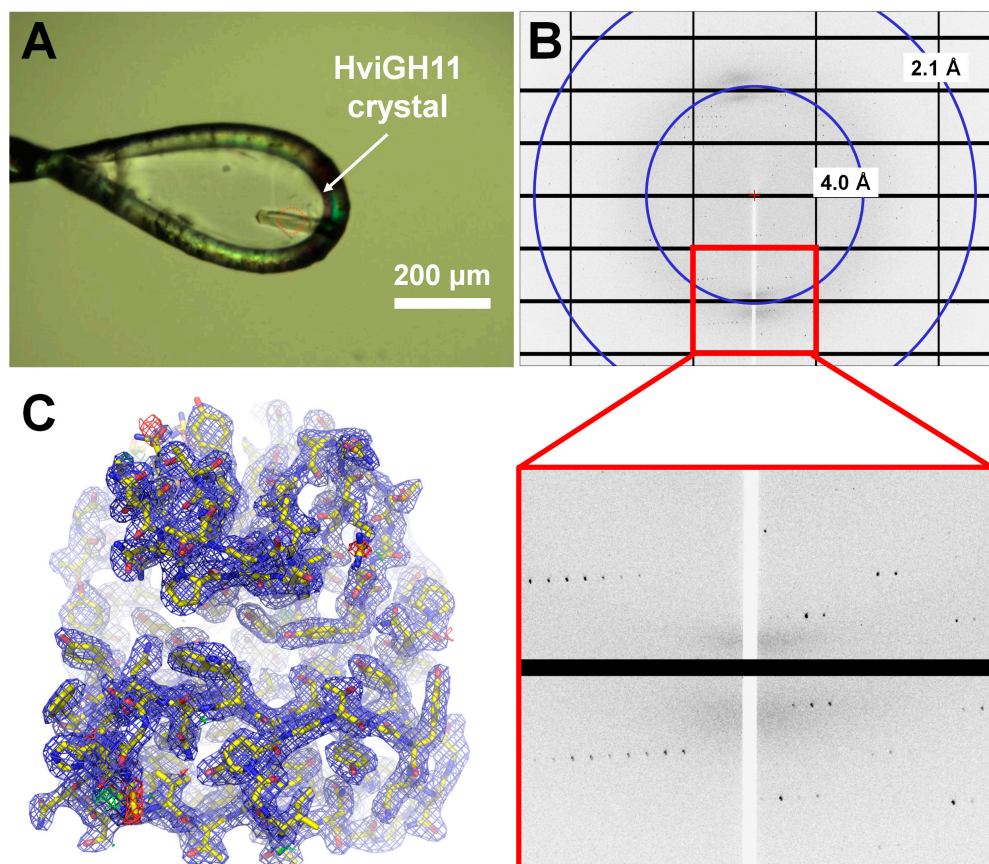


**Figure 3.** X-ray diffraction experiment and electron density map of HviGH11. (A) A photograph of the HviGH11 crystal mounted on a nylon loop during data collection. The X-ray exposure position is at the center of the red dot circle. (B) The diffraction pattern of an HviGH11 crystal optimized by adding PEG 4000. (C) 2mFo-DFc (blue mesh,  $1.0\sigma$ ) and mFo-DFc (green mesh,  $3\sigma$ ; red mesh,  $-3\sigma$ ) electron density map of HviGH11.

**Table 1.** Data collection statistics.

Data	PEG 400	PEG 4000	PEG 8000
Temperature (K)	100	100	100
Wavelength (Å)	0.9864	0.9864	0.9864
Space group	$P_{2_1}2_12_1$	$P_{2_1}2_12_1$	$P_{2_1}2_12_1$
Unit cell (Å)			
a	42.967	43.333	43.367
b	51.301	51.278	51.437
c	94.665	94.443	95.774
Resolution (Å)	50.00–2.10 (2.14–2.10)	50.00–1.95 (1.98–1.95)	50.00–2.40 (2.44–2.40)
Unique reflections	11,677 (517)	15,684 (778)	8283 (405)
Completeness (%)	91.2 (81.7)	97.6 (97.7)	97.1 (97.4)
Redundancy	5.0 (4.2)	5.0 (4.7)	3.8 (3.7)
Mean $I/\sigma(I)$	11.04 (2.04)	9.00 (1.90)	9.34 (1.94)
Rmerge	0.134 (0.506)	0.130 (0.595)	0.180 (0.582)

**Table 1.** Cont.

Data	PEG 400	PEG 4000	PEG 8000
CC1/2	0.997 (0.829)	0.993 (0.811)	0.956 (0.717)
CC*	0.952 (0.952)	0.998 (0.946)	0.989 (0.914)

Values in parentheses are for the outer shells.

The phase problem was successfully solved using the molecular replacement method, and a high-quality electron density map was obtained (Figure 3C). Model refinement is currently underway, and the crystal structure will be published separately.

#### 4. Discussion

HviGH11 microcrystals grew spontaneously after protein purification and concentration but showed poor X-ray diffraction at the synchrotron and XFEL facilities [24]. To prevent the spontaneous crystal growth of HviGH11, various crystallization factors such as temperature, pH, and salt concentration were examined to improve protein solubility and prevent spontaneous crystallization. However, these factors did not significantly improve the solubility of HviGH11 protein under different buffer conditions. Microcrystals formed spontaneously in all different protein solutions at 4 °C or room temperature. These results suggest that temperature, pH, and salt concentration do not play a significant role in preventing the protein–protein interactions of HviGH11 in solution or in crystal packing during the spontaneous crystal growth process. Furthermore, HviGH11 consistently produced numerous microcrystals of similar size under different spontaneous crystal growth conditions. These crystal screening studies often yielded relatively larger crystals than in previous experiments, but the diffraction intensities of all crystals did not reach a sufficient resolution to determine the protein structure.

Temperature, pH, and salt concentration did not affect protein solubility sufficiently to prevent the spontaneous crystal growth of HviGH11, but each of these factors clearly has the potential to affect solubility prior to spontaneous protein crystallization. Accordingly, to further understand the control of spontaneous growth crystallization, solubility experiments should be performed to understand how each factor affected the protein solution before crystal growth.

Meanwhile, in this study, the protein solution was filtered or centrifuged to remove aggregation or the presence of the nucleus before the protein crystallization process. However, it is possible that the nucleus was not completely removed and may remain in the protein solution used for crystallization.

In general, a precipitant promotes nucleation by inducing protein aggregation, and the number of crystals increases with an increasing concentration of the precipitant [35]. In contrast, when PEG was added as a precipitate to the concentrated HviGH11 solution, the number of crystals decreased and large crystals formed. This experimental result can be explained by considering the three-dimensional nucleation rate in the crystallization equation [36–38].

$$I = \frac{\text{const}}{\eta} \times C \times \left( -\frac{16\pi\gamma^3}{3kT(\Delta\mu)^2} \right)$$

where  $\eta$  is the viscosity,  $C$  is the solution concentration,  $\gamma$  is the surface tension, and  $\Delta\mu$  is the chemical potential difference between the crystal and the solution of a unit volume. According to this equation, the rate of three-dimensional nucleation increases at high protein concentration ( $C$ ), low viscosity ( $\eta$ ), low interfacial tension ( $\gamma$ ), and high chemical potential ( $\Delta\mu$ ). With highly viscous crystallization reagents such as PEG, the number of crystals decreases significantly with increasing viscosity ( $\eta$ ). Based on the results of this experiment, it was concluded that the addition of PEG reagent to the HviGH11 solution resulted in the formation of larger crystals. It is believed that the PEG reagent increases the viscosity of the solution rather than promoting nucleation, resulting in the suppression of nucleation. This conclusion is supported by the fact that higher viscosity is often associated

with reduced nucleation rates in crystallization processes [38,39]. For example, a previous lysozyme crystallization study showed that a small number of large lysozyme crystals were obtained in a crystallization solution containing 5% PEG 4000 and 0.2 M NaCl. However, when the concentration of PEG 4000 was increased to 15%, cluster crystals were observed. When grown in 20% PEG 4000 and 0.1 M NaCl, clustered crystals initially formed, but significantly larger crystals were obtained. Crystals grown at higher concentrations of PEG 4000 show higher-resolution diffraction [39]. Viscosity can affect the nucleation rate and number of HviGH11 crystals. Other viscous glycerols were also used to optimize HviGH11 crystal size, but no suitable crystals were obtained, even in the presence of microcrystals. These results indicate that the type of viscous precipitation solution is also an important factor in controlling the nucleation rate and number of HviGH11 crystals.

In these experiments, different weights and concentrations of PEG produced crystals of similar quality, indicating that the properties of the various PEGs did not play a significant role in the saturation of the protein. This indicated the influence on the number and size of crystals may be linked to the reduction of convection mass transport due to the increase in viscosity.

Based on the experimental crystallization results, the following crystallization process was proposed for HviGH11 (Figure 4). First, HviGH11 spontaneously undergoes a large number of nucleations within a certain period of time, and then the surrounding proteins are packed into the nucleation to grow crystals. In this case, the proteins were packed into multiple nuclei in solution and grew into many microcrystals that did not undergo X-ray diffraction (Figure 4). However, when the PEG precipitant was added, the effect of slowing the nucleation rate by increasing the viscosity of the crystallization solution was greater than promoting nucleation due to HviGH11 protein aggregation (Figure 4). This slow nucleation rate reduced the number of nucleations while simultaneously causing the growth of large crystals. Meanwhile, it was clearly observed that the number of nucleations was reduced due to the viscosity of PEG, resulting in large crystals. However, it is also possible that PEG contributed to the growth of large crystals by inducing nucleation faster than spontaneous crystal growth. To conclusively prove this, further studies are required to observe crystal growth through real-time monitoring.

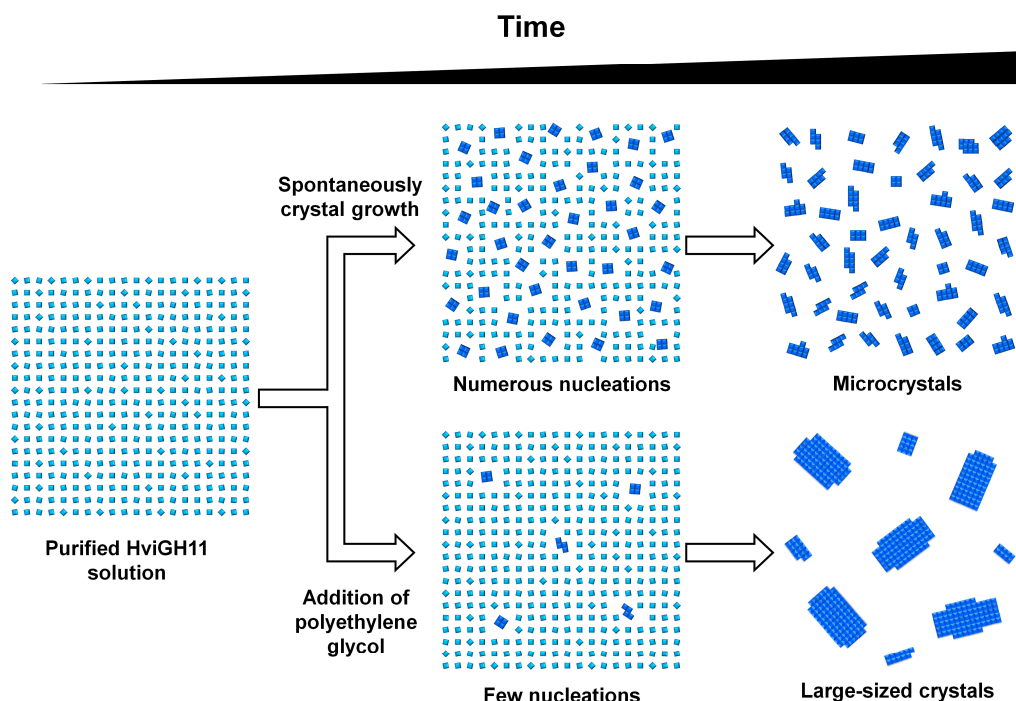


**Figure 4.** The proposed crystallization method to increase the size of spontaneously grown HviGH11 crystals using PEG agents. (Top) The crystallization process of spontaneously grown HviGH11. Multiple

nucleations occur at a specific time, and microcrystals form around multiple nucleations. (**Bottom**) Large crystal growth process of HviGH11 by adding PEG agents. The PEG precipitant increases the viscosity of the crystallization solution, reduces the number of nucleations, and grows large HviGH11 crystals with a low number of nucleations.

## 5. Conclusions

Here, factors that can improve the quality of spontaneously growing protein crystals that are of poor quality for acquiring complete diffraction data were investigated. By adding PEG reagent to the HviGH11 protein, which can spontaneously form crystals, the size of the crystals was improved, and complete high-resolution diffraction data were collected. Rather than contributing to increased protein crystal nucleation, PEG may have reduced crystal nucleation by increasing viscosity. These results will help advance our knowledge in protein crystallography and spontaneous crystal growth studies.

**Funding:** This work was funded by the National Research Foundation of Korea (NRF) (NRF-2021R1I1A1A01050838).

**Institutional Review Board Statement:** Not applicable.

**Informed Consent Statement:** Not applicable.

**Data Availability Statement:** Data are contained within the article.

**Acknowledgments:** We thank the staff at the 11C beamline at Pohang Accelerator Laboratory for their assistance with data collection.

**Conflicts of Interest:** The authors declare no conflicts of interest.

## References

1. McPherson, A.; Cudney, B. Optimization of crystallization conditions for biological macromolecules. *Acta Crystallogr. F Struct. Biol. Commun.* **2014**, *70*, 1445–1467. [[CrossRef](#)]
2. Durbin, S.D.; Feher, G. Protein Crystallization. *Annu. Rev. Phys. Chem.* **1996**, *47*, 171–204. [[CrossRef](#)] [[PubMed](#)]
3. McPherson, A. Protein Crystallization. In *Protein Crystallography; Methods in Molecular Biology*; Humana Press: New York, NY, USA, 2017; pp. 17–50.
4. Kendrew, J.C.; Bodo, G.; Dintzis, H.M.; Parrish, R.G.; Wyckoff, H.; Phillips, D.C. A Three-Dimensional Model of the Myoglobin Molecule Obtained by X-ray Analysis. *Nature* **1958**, *181*, 662–666. [[CrossRef](#)] [[PubMed](#)]
5. Schönherr, R.; Rudolph, J.M.; Redecke, L. Protein crystallization in living cells. *Biol. Chem.* **2018**, *399*, 751–772. [[CrossRef](#)] [[PubMed](#)]
6. Oeda, K.; Inouye, K.; Ibuchi, Y.; Oshie, K.; Shimizu, M.; Nakamura, K.; Nishioka, R.; Takada, Y.; Ohkawa, H. Formation of crystals of the insecticidal proteins of *Bacillus thuringiensis* subsp. *aizawai* IPL7 in *Escherichia coli*. *J. Bacteriol.* **1989**, *171*, 3568–3571. [[CrossRef](#)] [[PubMed](#)]
7. Fan, G.Y.; Maldonado, F.; Zhang, Y.; Kincaid, R.; Ellisman, M.H.; Gastinel, L.N. In vivo calcineurin crystals formed using the baculovirus expression system. *Microsc. Res. Tech.* **1996**, *34*, 77–86. [[CrossRef](#)]
8. Stöger, E.; Parker, M.; Christou, P.; Casey, R. Pea Legumin Overexpressed in Wheat Endosperm Assembles into an Ordered Paracrystalline Matrix. *Plant Physiol.* **2001**, *125*, 1732–1742. [[CrossRef](#)]
9. Hasegawa, H.; Wendling, J.; He, F.; Trilisky, E.; Stevenson, R.; Franey, H.; Kinderman, F.; Li, G.; Piedmonte, D.M.; Osslund, T.; et al. In Vivo Crystallization of Human IgG in the Endoplasmic Reticulum of Engineered Chinese Hamster Ovary (CHO) Cells. *J. Biol. Chem.* **2011**, *286*, 19917–19931. [[CrossRef](#)]
10. Gati, C.; Bourenkov, G.; Klinge, M.; Rehders, D.; Stellato, F.; Oberthür, D.; Yefanov, O.; Sommer, B.P.; Mogk, S.; Duszenko, M.; et al. Serial crystallography on in vivo grown microcrystals using synchrotron radiation. *IUCrJ* **2014**, *1*, 87–94. [[CrossRef](#)]
11. Coulibaly, F.; Chiu, E.; Ikeda, K.; Gutmann, S.; Haebel, P.W.; Schulze-Briese, C.; Mori, H.; Metcalf, P. The molecular organization of cypovirus polyhedra. *Nature* **2007**, *446*, 97–101. [[CrossRef](#)]
12. Chiu, E.; Hijnen, M.; Bunker, R.D.; Boudes, M.; Rajendran, C.; Aizel, K.; Oliéric, V.; Schulze-Briese, C.; Mitsuhashi, W.; Young, V.; et al. Structural basis for the enhancement of virulence by viral spindles and their in vivo crystallization. *Proc. Natl. Acad. Sci. USA* **2015**, *112*, 3973–3978. [[CrossRef](#)]
13. Schönherr, R.; Klinge, M.; Rudolph, J.M.; Fita, K.; Rehders, D.; Lübbert, F.; Schneegans, S.; Majoul, I.V.; Duszenko, M.; Betzel, C.; et al. Real-time investigation of dynamic protein crystallization in living cells. *Struct. Dyn.* **2015**, *2*, 041712. [[CrossRef](#)]
14. Colletier, J.-P.; Sawaya, M.R.; Gingery, M.; Rodriguez, J.A.; Cascio, D.; Brewster, A.S.; Michels-Clark, T.; Hice, R.H.; Coquelle, N.; Boutet, S.; et al. De novo phasing with X-ray laser reveals mosquito larvicide BinAB structure. *Nature* **2016**, *539*, 43–47. [[CrossRef](#)]

15. Gati, C.; Oberthuer, D.; Yefanov, O.; Bunker, R.D.; Stellato, F.; Chiu, E.; Yeh, S.-M.; Aquila, A.; Basu, S.; Bean, R.; et al. Atomic structure of granulin determined from native nanocrystalline granulovirus using an X-ray free-electron laser. *Proc. Natl. Acad. Sci. USA* **2017**, *114*, 2247–2252. [[CrossRef](#)]
16. Redecke, L.; Nass, K.; DePonte, D.P.; White, T.A.; Rehders, D.; Barty, A.; Stellato, F.; Liang, M.; Barends, T.R.M.; Boutet, S.; et al. Natively Inhibited Trypanosoma brucei Cathepsin B Structure Determined by Using an X-ray Laser. *Science* **2013**, *339*, 227–230. [[CrossRef](#)]
17. Nam, K.H.; Kim, S.-J.; Hwang, K.Y. Crystal structure of CelM2, a bifunctional glucanase–xylanase protein from a metagenome library. *Biochem. Biophys. Res. Commun.* **2009**, *383*, 183–186. [[CrossRef](#)]
18. Nam, K.H.; Lee, W.H.; Rhee, K.H.; Hwang, K.Y. Structural characterization of the bifunctional glucanase–xylanase CelM2 reveals the metal effect and substrate-binding moiety. *Biochem. Biophys. Res. Commun.* **2010**, *391*, 1726–1730. [[CrossRef](#)] [[PubMed](#)]
19. Paës, G.; Berrin, J.-G.; Beaugrand, J. GH11 xylanases: Structure/function/properties relationships and applications. *Biotechnol. Adv.* **2012**, *30*, 564–592. [[CrossRef](#)]
20. Kim, I.J.; Kim, S.R.; Kim, K.H.; Bornscheuer, U.T.; Nam, K.H. Characterization and structural analysis of the endo-1,4- $\beta$ -xylanase GH11 from the hemicellulose-degrading *Thermoanaerobacterium saccharolyticum* useful for lignocellulose saccharification. *Sci. Rep.* **2023**, *13*, 17332. [[CrossRef](#)] [[PubMed](#)]
21. Collins, T.; Gerday, C.; Feller, G. Xylanases, xylanase families and extremophilic xylanases. *FEMS Microbiol. Rev.* **2005**, *29*, 3–23. [[CrossRef](#)] [[PubMed](#)]
22. Walia, A.; Guleria, S.; Mehta, P.; Chauhan, A.; Parkash, J. Microbial xylanases and their industrial application in pulp and paper biobleaching: A review. *3 Biotech* **2017**, *7*, 11. [[CrossRef](#)]
23. Kim, I.J.; Kim, S.R.; Bornscheuer, U.T.; Nam, K.H. Engineering of GH11 Xylanases for Optimal pH Shifting for Industrial Applications. *Catalysts* **2023**, *13*, 1405. [[CrossRef](#)]
24. Nam, K.H.; Park, S.; Park, J. Preliminary XFEL data from spontaneously grown endo-1,4- $\beta$ -xylanase crystals from Hypocrea virens. *Acta Crystallogr. F Struct. Biol. Commun.* **2022**, *78*, 226–231. [[CrossRef](#)]
25. Gu, D.H.; Eo, C.; Hwangbo, S.A.; Ha, S.C.; Kim, J.H.; Kim, H.; Lee, C.S.; Seo, I.D.; Yun, Y.D.; Lee, W.; et al. BL-11C Micro-MX: A high-flux microfocus macromolecular-crystallography beamline for micrometre-sized protein crystals at Pohang Light Source II. *J. Synchrotron Radiat.* **2021**, *28*, 1210–1215. [[CrossRef](#)]
26. Otwinowski, Z.; Minor, W. Processing of X-ray diffraction data collected in oscillation mode. *Methods Enzymol.* **1997**, *276*, 307–326. [[CrossRef](#)]
27. Vagin, A.; Teplyakov, A. Molecular replacement with MOLREP. *Acta Crystallogr. D Biol. Crystallogr.* **2010**, *66*, 22–25. [[CrossRef](#)]
28. Jumper, J.; Evans, R.; Pritzel, A.; Green, T.; Figurnov, M.; Ronneberger, O.; Tunyasuvunakool, K.; Bates, R.; Žídek, A.; Potapenko, A.; et al. Highly accurate protein structure prediction with AlphaFold. *Nature* **2021**, *596*, 583–589. [[CrossRef](#)] [[PubMed](#)]
29. Murshudov, G.N.; Skubak, P.; Lebedev, A.A.; Pannu, N.S.; Steiner, R.A.; Nicholls, R.A.; Winn, M.D.; Long, F.; Vagin, A.A. REFMAC5 for the refinement of macromolecular crystal structures. *Acta Crystallogr. D Biol. Crystallogr.* **2011**, *67*, 355–367. [[CrossRef](#)] [[PubMed](#)]
30. McPherson, A.; Gavira, J.A. Introduction to protein crystallization. *Acta Crystallogr. F Struct. Biol. Commun.* **2013**, *70*, 2–20. [[CrossRef](#)]
31. Inyang, U.E.; Iduh, A.O. Influence of pH and salt concentration on protein solubility, emulsifying and foaming properties of sesame protein concentrate. *J. Am. Oil Chem. Soc.* **1996**, *73*, 1663–1667. [[CrossRef](#)]
32. Oeller, M.; Kang, R.; Bell, R.; Ausserwöger, H.; Sormanni, P.; Vendruscolo, M. Sequence-based prediction of pH-dependent protein solubility using CamSol. *Brief. Bioinform.* **2023**, *24*, bbad004. [[CrossRef](#)]
33. Dumetz, A.C.; Snellinger-O'Brien, A.M.; Kaler, E.W.; Lenhoff, A.M. Patterns of protein-protein interactions in salt solutions and implications for protein crystallization. *Protein Sci.* **2007**, *16*, 1867–1877. [[CrossRef](#)]
34. Rajan, R.; Ahmed, S.; Sharma, N.; Kumar, N.; Debas, A.; Matsumura, K. Review of the current state of protein aggregation inhibition from a materials chemistry perspective: Special focus on polymeric materials. *Mater. Adv.* **2021**, *2*, 1139–1176. [[CrossRef](#)]
35. Dessau, M.A.; Modis, Y. Protein Crystallization for X-ray Crystallography. *J. Vis. Exp.* **2011**, *47*, e2285. [[CrossRef](#)]
36. Manuel García-Ruiz, J. Nucleation of protein crystals. *J. Struct. Biol.* **2003**, *142*, 22–31. [[CrossRef](#)]
37. Yoshizaki, I.N.H.; Fukuyama, S.; Komatsu, H.; Yoda, S. Estimation of crystallization boundary of a model protein as a function of solute concentration and experiment time. *Int. J. Microgravity Sci. Appl.* **2002**, *19*, 30–33. [[CrossRef](#)]
38. Hashizume, Y.; Inaka, K.; Furubayashi, N.; Kamo, M.; Takahashi, S.; Tanaka, H. Methods for Obtaining Better Diffractive Protein Crystals: From Sample Evaluation to Space Crystallization. *Crystals* **2020**, *10*, 78. [[CrossRef](#)]
39. Takahashi, S.; Yan, B.; Furubayashi, N.; Inaka, K.; Tanaka, H. Effects of polyethylene glycol 4000 and Sodium chloride: 3-dimensional phase diagram for a protein crystallization. *Mater. Struct.* **2016**, *23*, 154.

**Disclaimer/Publisher's Note:** The statements, opinions and data contained in all publications are solely those of the individual author(s) and contributor(s) and not of MDPI and/or the editor(s). MDPI and/or the editor(s) disclaim responsibility for any injury to people or property resulting from any ideas, methods, instructions or products referred to in the content.